Constraining of Small-Ring Cyclic Ether Triads by Stereodefined Spiroannulation to an Inositol Orthoformate Platform. Solution- and Gas-Phase Alkali Metal Binding Affinities for Three- to Five-Membered Ring Structural Combinations

Leo A. Paquette,*[,†] Choon Sup Ra,[†,§] Judith C. Gallucci,[†] Ho-Jung Kang,[†,⊥] Naoki Ohmori,[†,||] Mark P. Arrington,[†] Wendi David,[‡] and Jennifer S. Brodbelt*[,‡]

The Evans Chemical Laboratories, The Ohio State University, Columbus, Ohio 43210, and Department of Chemistry and Biochemistry, The University of Texas at Austin, Austin, Texas 78712

paquette.1@osu.edu

Received July 25, 2001

The structural features most conducive to complexation of the alkali metal ions Li^+, Na^+, and K^+ in a series of constrained inositol orthoformate derivatives have been probed in solution, in the solid state, and in the gas phase by electrospray ionization mass spectrometry. The eight spirotricyclic polyethers differ in the size of the rings containing the potentially ligating oxygen atoms. Although the ring sizes have been limited to three to five atoms inclusively, the combinations of oxirane, oxetane, and tetrahydrofuran are rather extensive and consist of many options. The overall trend for lithium ion affinity is [5.5.5] > [5.5.4] > [4.4.4] > [5.5.3] > [5.4.3] > [4.4.3] > [1.1.1] > [3.3.1], an ordering that correlates with the differing polarizabilities of the oxygen atoms, ease of alignment of the nonbonded electron pairs, and the overall size of the ligand as gauged by nonbonded O·····O distances.

The striking capability of crown ethers to sequester metal cations while in solution has stimulated the examination of their potential to serve as delivery agents for the transport of ionic species to specific binding sites in living tissues.[1] The structures of such ligands and their complexes have been defined in the solid state,[2] in solution,[3] and at the theoretical level via molecular mechanics.[4] More recently, electrospray mass spectrometry has been applied to the determination of binding constants in the gas phase.[5] While it is recognized that structural parameters related to cavity size, number of ether oxygen atoms, length of carbon chain interconnecting the heteroatomic sites, and conformational flexibility individually impact on complex stability, the ensemble of factors that control metal ion recognition remain incompletely understood.

We recently introduced the conformationally constrained tris(spirotetrahydrofuran) ligands **1** as representatives of a potentially versatile new type of ionophore.[6] By taking advantage of the unique characteristics

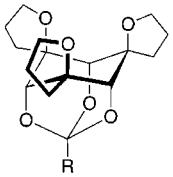

1a, R = H
b, R = CH_2OH
c, R = C≡CH

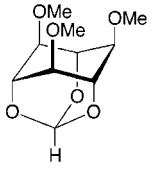

2

provided by *myo*-inositol ortho esters, it becomes possible to position the spiro ether oxygens 2.83 Å apart (X-ray analysis of **1a**). The result is an impressive selectivity for Li^+ over Na^+ and a high preference to form a 2:1 complex with lithium ion. In addition, **1c** is amenable to Glaser coupling with formation of a bifacial ligand that lends itself to formation of a rodlike polymer in the presence of Li^+. In the case of **2**, the methoxyl oxygens

† The Ohio State University.
‡ The University of Texas at Austin.
§ On leave from the Department of Chemistry, Yeungnam University, Kyongsan 712-749, Korea.
⊥ On leave from the Department of Chemistry, Kyunghee University, Seoul 130-701, Korea.
|| Visiting graduate student on leave from the Department of Chemistry, Hiroshima University, 1999-2000.

(1) Kozak, R. W.; Waldman, T. A.; Atcher, R. W.; Gansow, O. A. *Trends Biotechnol.* **1985**, *4*, 259.

(2) (a) Hilgenfeld, R.; Saenger, W. *Top. Curr. Chem.* **1982**, *101*, 1. (b) Dobler, M. *Ionophores and Their Structures*; Wiley-Interscience: New York, 1981.

(3) (a) Gokel, G. W. *Crown Ethers and Cryptands*; The Royal Society of Chemistry: Cambridge, England, 1991. (b) Cooper, S. R., Ed. *Crown Compounds: Toward Future Applications*; VCH Publishers: New York, 1992. (c) Vögtle, F. *Supramolecular Chemistry*; John Wiley and Sons: Chichester, England, 1991. (d) Inoue, Y.; Gokel, G. W. *Cation Binding by Macrocycles*; Marcel Dekker: New York, 1990. (e) Westley, W. J., Ed. *Polyether Antibiotics*; Marcel Dekker: New York, 1983; Vols. I and II. (f) Izatt, R. M.; Christensen, J. J. *Synthetic Multidentate Macrocyclic Compounds*; Academic Press: New York, 1978.

(4) (a) Hay, B. P.; Rustad, J. R.; Hostetler, C. J. *J. Am. Chem. Soc.* **1993**, *115*, 11158. (b) Hay, B. P.; Rustad, J. R. *J. Am. Chem. Soc.* **1994**, *116*, 6316 and relevant references therein.

(5) (a) Kempen, E. C.; Brodbelt, J. S. *Anal. Chem.* **2000**, *72*, 5411. (b) Ryzhov, V.; Dunbar, R. C.; Cerda, B.; Wesdemiotis C. *J. Am. Soc. Mass Spectrom.* **2000**, *11*, 1037. (c) Madhusudanan, K. P.; Raj, K.; Bhaduri, A. P. *Rapid Commun. Mass Spectrom.* **2000**, *14*, 885. (d) Goolsby, B. J.; Brodbelt, J. S.; Adou, E.; Blanda, M. *Intern. J. Mass. Spectrom.* **1999**, *193*, 197. (e) Kempen, E. C.; Brodbelt, J. S.; Bartsch, R. A.; Jang, Y.; Kim, J. S. *Anal. Chem.* **1999**, *71*, 5493. (f) Cerda, B. A.; Hoyau, S.; Ohanessian, G.; Wesdemiotis, C. *J. Am. Chem. Soc.* **1998**, *120*, 2437. (g) Cerda, B. A.; Wedesmiotis, C. *J. Am. Chem. Soc.* **1996**, *118*, 11884. (h) Blair, S. M.; Brodbelt, J. S.; Marchand, A. P.; Kalpencherry, A.; Chong, H.-S. *Anal. Chem.* **2000**, *72*, 2433. (i) Blair, S. M.; Brodbelt, J. S.; Madhusudhan Reddy, G.; Marchand, A. P. *J. Mass Spectrom.* **1998**, *33*, 721.

(6) (a) Tae, J.; Rogers, R. D.; Paquette, L. A. *Org. Lett.* **2000**, *2*, 139. (b) Paquette, L. A.; Tae, J.; Gallucci, J. C. *Org. Lett.* **2000**, *2*, 143. (c) Paquette, L. A.; Tae, J. *J. Am. Chem. Soc.* **2001**, *123*, 4974.

10.1021/jo0107507 CCC: $20.00
Published on Web 11/14/2001

have been found by crystallographic means to reside at distances ranging from 2.88 to 2.96 Å. Notwithstanding, this particular syn noncyclic arrangement is not conducive to binding to any alkali metal ion in solution.

Rather surprisingly, relatively little effort has been devoted to exploring how changes in the nature of the ether oxygen (i.e., the contrast between **1a** and **2**) affects the strength and selectivity with which oxophilic metal ions become ligated. Also, minimal attention has been given to establishing the relationship, if any, between molecular symmetry and cation binding capability.[7] Although early work demonstrated a correlation between cavity radius and the size of alkali and alkaline earth metal ions,[8] later studies by Hancock and co-workers employing a wider variety of cations demonstrated the concept to have limited applicability.[9] The upshot of their investigation is that complexation properties should never be assumed and always directly measured. Finally, the natural progression from methoxy to oxirane and then to oxetane and tetrahydrofuran is well recognized to be accompanied by changes in basicity.[10] For example, oxetane is a stronger base than methyl ethyl ether.

With the above in mind, we became interested in a direct comparative analysis of a group of spatially well defined compounds closely related to **1** and **2**. The selection ranges from the C_{3v}-symmetric congeners **3** and **4** to the four C_s-symmetric trispiro ethers **5**−**8**, and ultimately to **9**, the only chiral member of this subset.

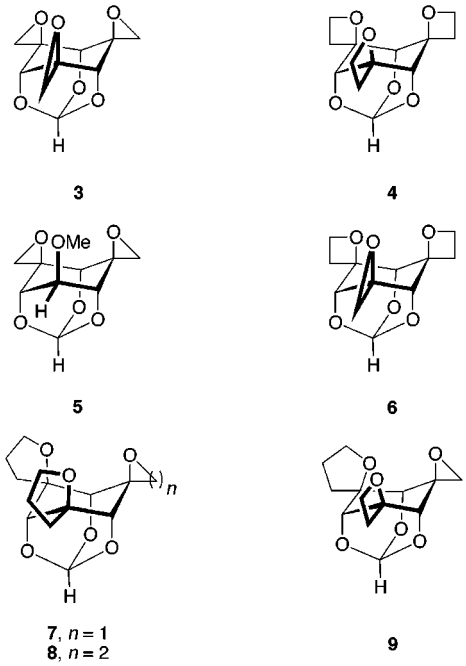

3 **4** **5** **6** **7**, $n = 1$ **8**, $n = 2$ **9**

For convenience, numerical descriptors will be used to define the sizes of the ether oxygen-containing, nonortho ester subunits. On this basis, **1a** is the [5.5.5] ionophore, the trimethoxy derivative **2** becomes the [1.1.1] analogue, and **5** and **9** will be referred to as the [3.3.1] and [5.4.3] ligands. Computational studies involving the MM3 force field suggest that as the size of the spiro ether ring decreases, the internuclear O·····O gap will increase. Less obvious is the degree of regularity of these changes. Different arrangements of the ligating oxygens in the host were nonetheless anticipated to have direct consequences on guest ion selectivities.

In the present study, the alkali metal binding properties of the new cyclic ether triads have been evaluated in solution by a picrate extraction method and by electrospray ionization-mass spectrometric (ESI-MS) methods. The latter technique has been used increasingly to evaluate aspects of molecular recognition on the basis of the formation of host−guest complexes in solution, followed by transport to the gas phase for mass spectrometric detection.[5,11] The intensities of complexes in the resulting mass spectra are used to estimate the relative binding selectivities of different hosts for different guests, and in general, these measurements correlate with the solution binding properties of the hosts and guests. This general method has been used previously to assess the alkali metal binding properties of a variety of macrocyclic hosts.[5,11] For evaluation of the gas-phase binding properties of hosts, a tandem mass spectrometric method coined "the kinetic method" is frequently used.[12] In this method, a heterodimer complex consisting of one molecule of each of two different organic compounds bound to a single cation (or anion) is formed in the gas phase and then subjected to collisional activation to promote the dissociation of the complex. Typically the complex dissociates by loss of either organic ligand, and the relative propensities for these two competing dissociation pathways are monitored on the basis of the intensities of the resulting fragment ions. Because the initial heterodimeric complexes and the resulting fragment ions are unsolvated, the results obtained from this experimental procedure reflect the gas-phase cation affinities of the two molecules in the complex. This method has been used to determine the gas-phase acidities and basicities of numerous organic compounds, in addition to metal cation affinities.[12] Because the trispirocyclic ethers in the present study were designed to selectively bind lithium, the lithium binding properties are the major focus of the mass spectrometric measurements.

Results and Discussion

Synthesis of the [3.3.3] and [3.3.1] Ligands. Our point of departure was the differentially functionalized ketone **10**, whose efficient four-step synthesis from *myo*-inositol has been detailed earlier.[6c] The known chemistry of this early intermediate has established that exo approach to the carbonyl group is very much kinetically preferred. Accordingly, there was every expectation that

(7) Liu, Y.; Inoue, Y.; Hakushi, T. *Bull. Chem. Soc. Jpn*. **1990**, *63*, 3044.

(8) Lamb, J. D.; Izatt, R. M.; Christensen, J. J.; Eatough, D. J. *Coordination Chemistry of Macrocyclic Compounds*; Melson, G. A., Ed.; Plenum Press: New York, 1979; pp 145−217.

(9) Hancock, R. D. *J. Chem. Ed*. **1992**, *69*, 615.

(10) Bordejé, M. C.; Mó, O.; Yáñez, M.; Herreros, M.; Abboud, J.-L. M. *J. Am. Chem. Soc*. **1993**, *115*, 7389.

(11) (a) Jorgensen, T. J. D.; Roepstorff, P.; Heck, A. J. R. *Anal. Chem*. **1998**, *70*, 4427. (b) Jorgensen, T. J. D.; Staroske, T.; Roepstorff, P.; Williams, D. H.; Heck, A. J. R. *J. Chem. Soc., Perkin Trans. 2* **1999**, 1859. (c) Leize, E.; Jaffrezic, A.; Van Dorsselaer, A. *J. Mass Spectrom*. **1996**, *31*, 537. (d) Wang, K.; Gokel, G. W. *J. Org. Chem*. **1996**, *61*, 4693. (e) Young, D.-S.; Hung, H.-Y.; Liu, L. K. *J. Mass Spectrom*. **1997**, *32*, 432. (f) Blair, S. M.; Kempen, E. C.; Brodbelt, J. S. *J. Am. Soc. Mass Spectrom*. **1998**, *9*, 1049. (g) Brodbelt, J. S.; Kempen, E.; Reyzer, M. *Struct. Chem*. **1999**, *10*, 213. (h) Blair, S.; Brodbelt, J.; Marchand, A. P.; Chong, H.-S.; Alihodzic, S. *J. Am. Soc. Mass. Spectrom*. **2000**, *11*, 884. (i) Reyzer, M. L.; Brodbelt, J. S.; Marchand, A. P.; Chen, Z.; Huang, Z.; Namboothiri, I. N. N. *Int. J. Mass Spectrom*. **2001**, *204*, 133. (j) Kempen, E. C.; Brodbelt, J. S.; Bartsch R. A.; Blanda, M. T.; Farmer, D. B. *Anal. Chem*. **2001**, *73*, 384.

(12) Cooks, R. G.; Patrick, J. S.; Kotiaho, T.; McLuckey, S. A. *Mass Spectrom. Rev*. **1994**, *13*, 287.

Scheme 1

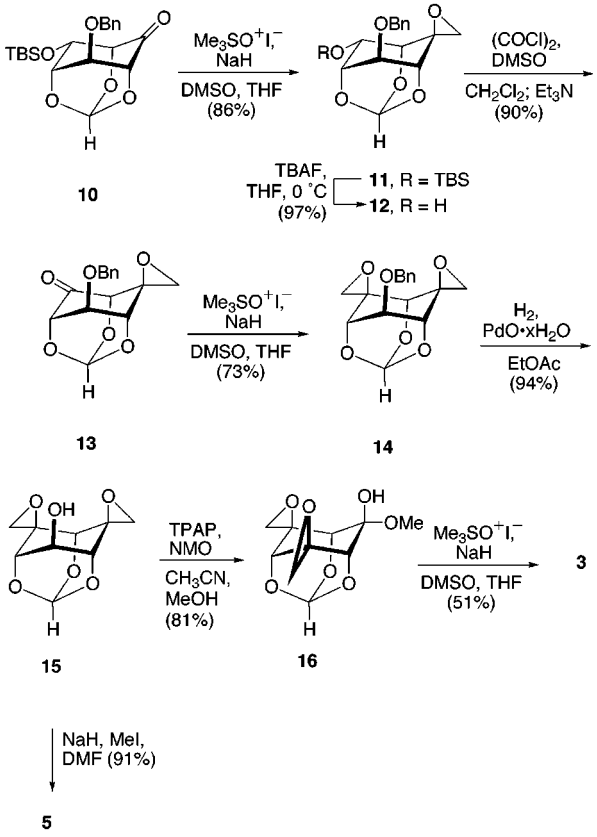

treatment of **10** with dimethylsulfoxonium methylide[13] would result in methylene transfer from the molecular exterior to deliver epoxide **11**. In practice, this isomer was produced exclusively (Scheme 1) as evidenced by the appearance of the pair of oxirane protons at unperturbed chemical shifts (δ 2.88 and 2.85 in $CDCl_3$) and ultimately an X-ray crystallographic analysis of **3**.

After the desilylation of **11** and Swern oxidation to deliver ketone **13**, use was again made of the sulfur ylide methylenation process. Although diepoxide **14** was uniquely formed, the efficiency of this conversion was approximately 13% less than that encountered on the first occasion. We consider nonbonded steric compression to be responsible.

In the preparation for the third capping maneuver, the benzyl group in **14** was cleaved via hydrogenolysis, thus making the axial alcohol directly available. This isomer was significantly less polar than its equatorial counterpart.[14] More importantly, **15** was amenable to oxidation, whereas its epimer was unreactive under comparable conditions. The exterior or interior placement of the carbinol proton is consequently an important structural feature in these systems. Its endo placement significantly deters the hydrogen abstraction process required for conversion to the ketonic product. While conventional *O*-methylation of **15** led efficiently to the [3.3.1] ligand **5**, alternative conversion to the [3.3.3] target mandated an initial change in oxidation level prior to introduction of the third oxiranyl unit. From among the several oxidants that were explored, tetra-*n*-propylammonium perruthenate[15] emerged as the most accommodating. This step was best carried out in a mixed acetonitrile/methanol solvent system, this combination resulting in the isolation of methyl hemiacetal **16**. Purification by recrystallization was thereby facilitated. The prospect of utilizing **16** directly in the third and final methylenation proved to be workable and to make **3** available. The significant number of crystalline intermediates en route to **3** make the sequence well suited to the production of reasonably large quantities as needed.

The single-crystal X-ray analysis of **3** (see Supporting Information) not only confirms the structural assignment, but provides important information concerning the interatomic distances between the three oxiranyl oxygens. In this instance, the O_1-O_2 and O_2-O_2* distances are 3.176 (2) and 3.162 (2) Å, respectively. These gaps are significantly larger than those adopted in the [5.5.5] example (see above).

Accessibility of the [4.4.3] and [4.4.4] Congeners. At this juncture, it became clear that diepoxide **14** could serve as a viable precursor to the oxetane-containing ligands **4** and **6**. We were pleased to discover that 2-fold structural ring expansion materializes simply by allowing **14** to react with approximately 4 equiv of dimethylsulfoxonium methylide at room temperature for 1 h. Under these reaction conditions, both epoxide rings undergo insertion of an additional CH_2 group with retention of stereochemistry at the associated C−O bonds[16,17] (Scheme 2). The best indicator of the success of this important transformation is the obvious retention of C_s symmetry as reflected in the ^1H and ^{13}C NMR spectra of **17**. Advancement to ketone **19** and hemiacetal **20** was next accomplished as before by sequential hydrogenolysis and perruthenate oxidation. The **19**/**20** ratio was found to be 1.6:1, indicating that the driving force to add methanol to the carbonyl group to be abated in the dioxetane series relative to its diepoxide congener.

Treatment of this mixture with an excess of the sulfur ylide resulted in successful conversion to the [4.4.4]

(13) Corey, E. J.; Chaykovsky, M. *J. Am. Chem. Soc.* **1965**, *87*, 1353.

(14) The exo alcohol **i** was easily obtained by the simple reversal of several steps as shown below. The elevated polarity and insolubility of **i** is particularly notable.

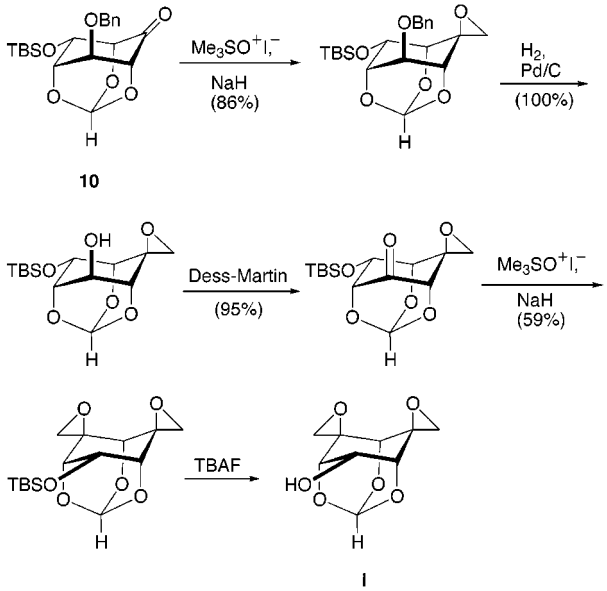

(15) Griffith, W. P.; Ley, S. V. *Aldrichim. Acta* **1990**, *23*, 13.

(16) Okuma, K.; Tanaka, Y.; Kaji, S.; Ohta, H. *J. Org. Chem.* **1983**, *48*, 5133.

(17) Fitton, A. O.; Hill, J.; Jane, D. E.; Millar, R. *Synthesis* **1987**, 1140.

Scheme 2

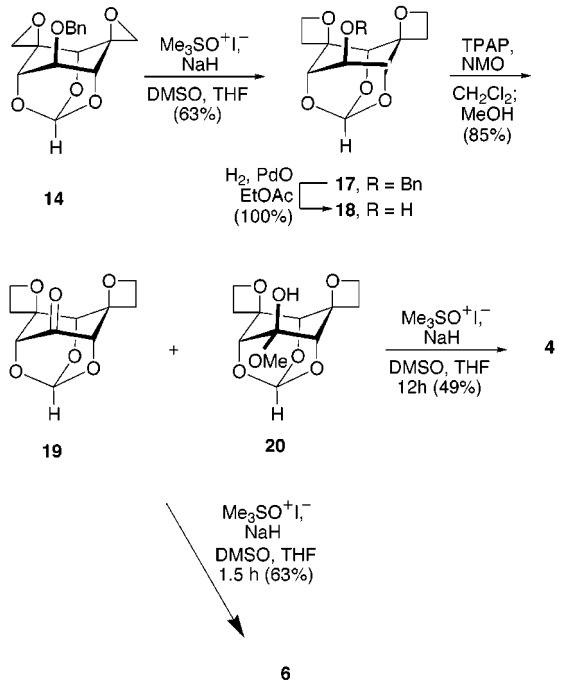

Scheme 3

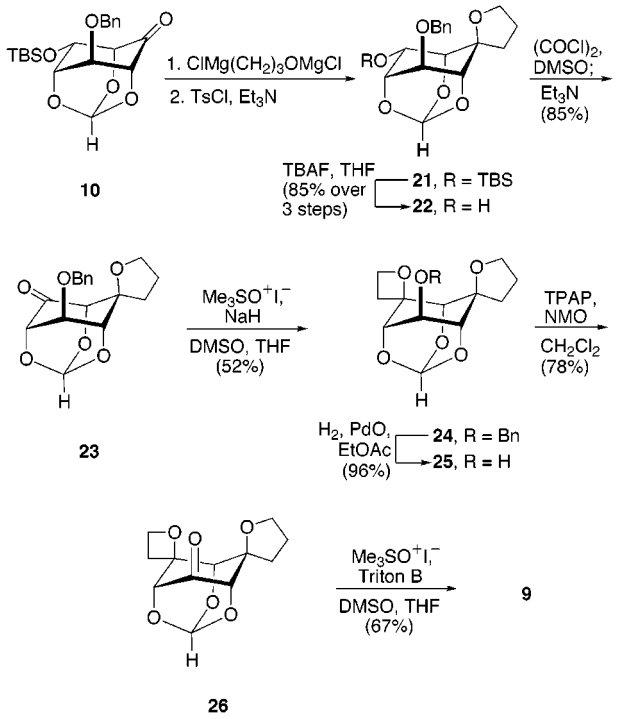

ligand **4**. On this basis, we anticipated that a reduction in the relative proportion of reactive ylide to only a slight excess would deliver the [4.4.3] triad. Indeed, a 63% yield of **6** was realized.

The crystal structure of **4** was also determined by single-crystal X-ray diffraction analysis (see Supporting Information). In the solid phase, the oxetanyl rings are seen to be canted to some degree away from the molecular interior. The resulting intramolecular O·····O distances are $O_1-O_2 = 3.051(2)$, $O_1-O_3 = 3.020(2)$, and $O_2-O_3 = 3.021(2)$ Å. These data confirm the anticipated existence of an incremental progression in the preorganizational characteristics of **1a**, **4**, and **3**, with the three oxygen atoms in the binding pocket of **1a** being the closest to each other.

Arrival at the Remaining Members of the Subset. In contemplating a workable route to the chiral [5.4.3] system **9**, we came to regard the most feasible pathway to be that in which the largest tetrahydrofuranyl ring would be installed first followed by the other two oxygen-containing rings in decreasing size. The preparation of ketone **23** from **10** as outlined in Scheme 3 therefore became our interim goal. As previously recognized,[6] building of the tetrahydrofuran by initial coupling to the Normant reagent[18] and subsequent dehydrative cyclization of the 1,4-diol so formed via tosylation proceeds in a secure way to set the desired configuration at the spirocyclic center in **21**. With this intermediate in hand, the *tert*-butyldimethylsilyloxy functionality was chemically modified in order to leave the remaining ether oxygen (as OBn) axially disposed. In fact, the two-step conversion of **21** to ketone **23** nicely set the stage for proper introduction of the oxetane ring via methodology developed earlier. Subsequently, compound **24** emerged as a proper precursor of the more structurally elaborated ketone **26**, whose conversion to **9** was readily accomplished.

(18) Cahiez, G.; Alexakis, A.; Normant, J. F. *Tetrahedron Lett.* **1978**, 3013.

Scheme 4

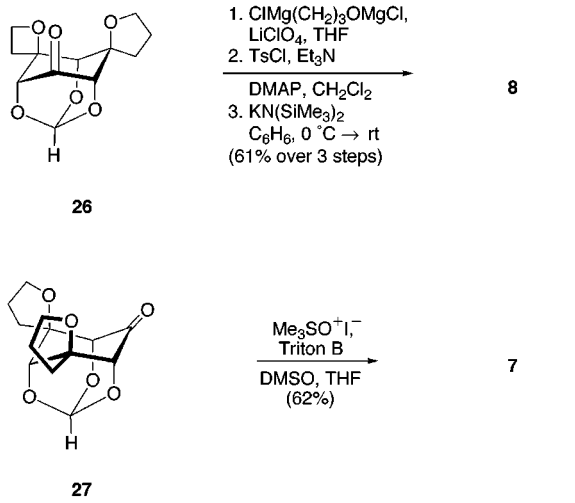

As shown in Scheme 4, ketone **26** gave rise to the [5.5.4] ligand in good yield when subjected to the Normant protocol. Equally successful was the conversion of **27**[6] to **7** in the presence of dimethylsulfoxonium methylide. Accordingly, the use in three central reactions has been shown to provide direct access to the seven target compounds defined in the Introduction. Possibilities for differentiating the various ring sizes have been identified, and optimal versions of these protocols are believed to have been established.

Solution-Phase Complexation Studies. The inositol orthoformate platform that serves as the common architectural component of **1**−**9** effectively reduces the population of available conformations and conveys considerable structural rigidity. The cation-binding properties of these potential hosts will consequently result in large part from the nonbonded oxygen−oxygen distances within the ionophoric cavity, differences in basicity, polarizability at the oxygen centers, and the like, rather than the

Table 1. Association Constants (K_a) Determined by Picrate Extraction from $CHCl_3$

ionophore	Li^+	Na^+	K^+
[3.3.1] (**5**)	2.3×10^4	3.4×10^4	3.7×10^4
[3.3.3] (**3**)[a]			
[4.4.3] (**6**)	3.8×10^3	2.2×10^4	3.2×10^4
[4.4.4] (**4**)	1.1×10^4	2.8×10^4	2.5×10^4
[5.4.3] (**9**)	7.0×10^3	2.2×10^4	1.7×10^4
[5.5.3] (**7**)	6.2×10^3	3.8×10^4	3.1×10^4
[5.5.4] (**8**)	1.2×10^6	2.1×10^4	2.9×10^3
[5.5.5] (**1a**)[b]	1.1×10^7	2.5×10^4	5.1×10^3

[a] K_a measurement was precluded by the low solubility of this ligand in chloroform. [b] Data taken from ref 6.

entropic and enthalpic costs that nonpreorganized systems must pay during the complexation process. When the latter conditions apply, solvent effects play a major role in ion selectivity. In the case of 18-crown-6, for example, the binding free energies in a variety of solvents are in the order $K^+ > Rb^+ > Cs^+ > Na^+ > Li^+$.[19] In contrast, theoretical estimates of the best binding enthalpies in the gas-phase drop off as $Li^+ > Na^+ > K^+ > Rb^+ > Cs^+$.[20] A priori, comparable crossover effects would not be anticipated in conformationally rigidified contexts, but ionophores of this type have received very limited attention.

Initially, the association constants K_a for the binding of Li^+, Na^+, and K^+ ions were determined in water/chloroform mixtures by means of Cram's picrate extraction method.[21] For calibration purposes, the K_a values for 12-crown-4 and 15-crown-5 were obtained for direct comparison with previous literature data.[21−25] The fact that **1**−**9** share in common a trio of oxygen-centered binding sites reasonably allows for direct comparisons to be made. Unfortunately, the very insoluble nature of the [3.3.3] compound precluded its evaluation in this manner. As previously recognized,[6] the donor atoms in the [5.5.5] ligand are spatially arranged in a manner that is notably conducive to satisfying the structural requirements for strong interaction with Li^+. A decrease in the size of one tetrahydrofuran ring to the oxetane level is met with a 10-fold reduction in the magnitude of K_a. Any more profound contraction of ring size in any of the three sectors clearly has deleterious consequences. Such a precipitous falloff in complexation capability was not originally anticipated.

As reflected in Table 1, the seven inositol-based ethers exhibited only weak affinity for Na^+ and K^+ ions. Therefore, progressive expansion of the nonbonded O·····O internuclear distances from 2.88 to 3.19 Å is not met with equivalent or enhanced alkali metal ion binding affinity, despite only modest changes in the relevant atomic radii of the cations (e.g., Li^+, 0.76 Å; Na^+, 1.02 Å).

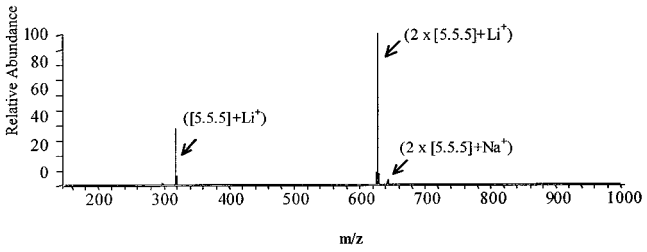

Figure 1. ESI-mass spectrum of [5.5.5] and LiCl in 99% $CHCl_3$.

The complexing capabilities of **2**−**9** were also probed by incremental titration of 1:1 $CH_3CN/CDCl_3$ solutions with $LiClO_4$ and concurrent inspection of possible changes in ^{13}C NMR chemical shifts.[26,27] Of the eight possible hosts, only the [5.5.4] example gave evidence of complexation. With this ligand, the formation of a 2:1 sandwich complex with Li^+ was clearly visible following the introduction of 0.5 molar equiv of the perchlorate salt. However, no further alterations in the spectral parameters were apparent up to the introduction of 1.0 equiv. The observations address the stability of the first-formed complex in the midst of excess Li^+. This behavior closely parallels the behavior of the [5.5.5] compound.[6c] In the case of the other analogues, modest changes in chemical shifts and peak intensities were observed, but absorptions due to a Li^+−host complex did not materialize.

Electrospray Ionization-Mass Spectrometry Gas-Phase Measurements. Four types of electrospray ionization-mass spectrometry (ESI-MS) experiments were undertaken to evaluate the metal complexation of the series of ionophores. The first entailed a procedure to screen the Li^+, Na^+, and K^+ metal complexation of each ligand in order to assess the types of complexes formed (i.e., 1:1, 2:1, and others), to evaluate the propensity for solvent adduction and counterion attachment, and to determine the overall signal intensity generated by each ligand. Solutions containing a single ligand and a single metal were prepared in 99% chloroform and analyzed by ESI-MS. Figure 1 shows the ESI-mass spectrum obtained for a solution containing [5.5.5] and LiCl. These first experiments showed that 1:1 and 2:1 complexes are readily detected in the ion trap mass spectrometer, indicating that they survive the ESI process. Complexes with solvent molecules, multiple metals, or counterions are not generally observed. A minor amount of Na^+ complexes are observed upon ESI of the Li^+ solutions as a result of the ubiquitous presence of Na^+ in the laboratory. All of the ligands, with the exception of [3.3.3], formed complexes with Li^+ and Na^+. Ligand [3.3.3] possesses three epoxide rings and may be more susceptible to spontaneous decomposition under the conditions for mass spectrometric analysis, or its poor solubility may render it undetectable. Note that [3.3.3] likewise was not amenable to evaluation by the picrate extraction method discussed earlier, a result attributed to its poor solubility. On the basis of the ESI-MS results for the solutions containing each ligand and a single metal, the ionophore/alkali metal complexes have similar ESI spray efficiencies, thus allowing facile comparison of the various complexes in later experiments.

(19) (a) Izatt, R. M.; Bradshaw, J. S.; Nielsen, S. A.; Lamb, J. D.; Christensen, J. J.; Sen, D. *Chem. Rev.* **1985**, *85*, 271. (b) Izatt, R. M.; Pawlak, K.; Bradshaw, J. S.; Bruening, R. L. *Chem. Rev.* **1991**, *91*, 1721. (c) The Na^+ and K^+ ordering is reversed in CH_3CN. De Jong, F.; Reinhoudt, D. N. *Adv. Phys. Org. Chem*. **1980**, *17*, 279.

(20) Glendening, E. D.; Feller, D.; Thompson, M. A. *J. Am. Chem. Soc.* **1994**, *116*, 10657.

(21) Koenig, K. E.; Lein, G. M.; Stuckler, P.; Kaneda, T.; Cram, D. J. *J. Am. Chem. Soc.* **1979**, *101*, 3553.

(22) Inoue, Y.; Amano, F.; Okada, N.; Inada, H.; Ouchi, M.; Tai, A.; Hakushi, T.; Lin, Y.; Tong, L.-H. *J. Chem. Soc., Perkin Trans. 2* **1990**, 1239.

(23) Paquette, L. A.; Negri, J. T.; Rogers, R. D. *J. Org. Chem*. **1992**, *57*, 3947.

(24) Erickson, S. D.; Still, W. C. *Tetrahedron Lett*. **1990**, *30*, 4253.

(25) Iimori, T.; Still, W. C.; Rheingold, A. L.; Staley, D. L. *J. Am. Chem. Soc.* **1989**, *111*, 3439.

(26) Hoffmann, R. W.; Münster, I. *Liebigs Ann./Recueil* **1997**, 1143.

(27) Paquette, L. A.; Tae, J.; Hickey, E. R.; Trego, W. E.; Rogers, R. D. *J. Org. Chem*. **2000**, *65*, 9160.

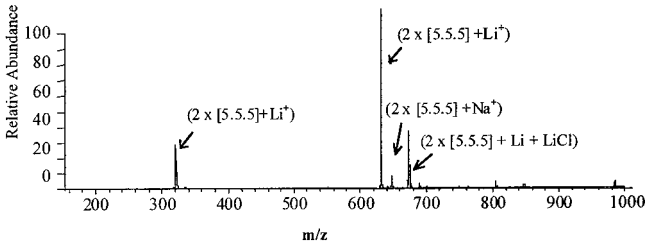

Figure 2. ESI-mass spectrum of [5.5.5] with LiCl, NaCl, and KCl in 99% $CHCl_3$.

The second type of experiment involved the determination of alkali metal binding selectivity for each ligand based on ESI-MS examination of solutions containing one ligand and three alkali metals (LiCl, NaCl, KCl each at 1×10^{-5} M). An example is shown in Figure 2 for [5.5.5]. In the resulting mass spectrum (Figure 2), both 1:1 and 2:1 (ligand:metal) complexes are observed, with the 2:1 complexes more dominant than the 1:1 complexes (as observed for most of the ligands). The K^+ complexes are always negligible. The relative intensities of the Li^+, Na^+, and K^+ complexes for each ligand were used to estimate the binding selectivities. Table 2 summarizes these results, along with the molecular weight and polarizability of each ligand. All of the ligands show the same trend in alkali metal binding selectivity: $Li^+ > Na^+ > K^+$. The selectivity for Li^+ over Na^+ varies somewhat from one ligand to another, but clearly all of these ligands have the greatest affinity for Li^+. The selectivity results shown in Table 1 for ligands **3**−**7** and **9** obtained by the picrate extraction method do not uniformly mirror the preference for Li^+ observed in the ESI-MS experiments shown in Table 2. This difference between the ESI-MS results and the picrate extraction results is attributed to solvation effects. In the picrate extraction method, the metals are initially solvated in a polar aqueous environment, and thus they must be desolvated upon transport to the chloroform phase. The extraction of Li^+, with the highest solvation energy, is the most energy-demanding process. In the ESI-MS measurements, both the ionophore and the metal ions are solvated in the same 99% chloroform/1% methanol environment, thus alleviating the impact of solvation effects on the complexation reactions.

The ESI-mass spectral results suggest that [5.5.5] is one of the most selective ionophores based on the intensity ratio for the Li^+ versus Na^+ complexes (i.e., 10:1 for the ([5.5.5] + Li^+) vs ([5.5.5] + Na^+) complexes), and a similar result was reflected from the picrate extraction experiments in Table 1. The ESI-MS results indicate that [5.5.3] and [4.4.3] are among the least selective ionophores with Li^+/Na^+ intensity ratios of ~2:1.

The third type of mass spectrometric experiment was aimed at evaluating the relative binding affinities of the series of ionophores and involved the ESI-MS analysis of solutions containing pairs of ligands (L1 and L2) and LiCl (no other metals), with the two ligands at equimolar concentrations (1×10^{-5} M) and LiCl at 2×10^{-5} M in 99% chloroform. An example is shown in Figure 3 for a solution containing [5.5.5] and [5.5.4] with LiCl. The relative binding affinities of the ligands were determined

Table 2. Alkali Metal Selectivities by ESI-MS[a]

compound mol wt polarizability[b]	metal	1:1 complex intensity[c]	2:1 complex intensity[d]	alkali metal selectivity (relative intensities for 1:1 and 2:1 complexes containing Li+ vs Na+)[d]
[5.5.5]	Li	very strong	very strong	Li>>Na >>> K
310	Na	moderate	moderate	(10:1)
29.3	K	very weak	none	(4:1)
[5.5.4]	Li	strong	very strong	Li > Na >>> K
296	Na	moderate	moderate	(5:1)
27.5	K	none	none	(2:1)
[5.5.3]	Li	strong	strong	Li > Na >>> K
282	Na	moderate	moderate	(3:1)
25.6	K	very weak	none	(1.5:1)
[4.4.4]	Li	strong	moderate	Li > Na >>> K
268	Na	moderate	moderate	(3:1)
23.8	K	none	none	(1:1)
[4.4.3]	Li	moderate	moderate	Li > Na >>> K
254	Na	moderate	moderate	(3:1)
22.0	K	very weak	none	(1:1)
[3.3.3]	Li	none	none	na[e]
226	Na	none	none	
18.3	K	none	none	
[3.3.1]	Li	weak	weak	Li > Na >>> K
228	Na	weak	weak	(1:1)
19.1	K	none	none	(0.3:1)
[5.4.3]	Li	moderate	moderate	Li > Na >>> K
268	Na	moderate	moderate	(2:1)
23.8	K	none	none	(1:1)
[1.1.1]	Li	strong	weak	Li > Na >>> K
232	Na	weak	weak	(8:1)
20.6	K	none	none	(1:1)

[a] For solutions containing 1:1:1:1 ligand:Li:Na:K in 99% chloroform/1% methanol. [b] Molecular weight in amu, polarizability in $Å^3$ calculated on the basis of atomic hybrid polarizability method.[29] [c] Qualitative indication of the mass spectral intensity of the 1:1 (ligand + metal)$^+$ and 2:1 (2 × ligand + metal)$^+$ complexes. [d] Comparison of the intensities of the (ligand + $Li)^+$ to (ligand + $Na)^+$ complexes and comparison of the intensities of the (2 × ligand + $Li)^+$ to (2 × ligand + $Na)^+$ complexes. [e] na = not applicable because complexes were not observed.

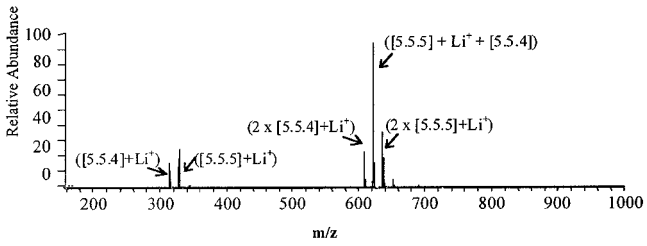

Figure 3. ESI-mass spectrum of [5.5.5] and [5.5.4] with LiCl in 99% $CHCl_3$.

on the basis of the intensities of the (L1 + Li^+) and (2 × L1 + Li^+) complexes and (L2 + Li^+) and (2 × L2 + Li^+) complexes in the resulting ESI-mass spectra, where (L1 + Li^+) and (L2 + Li^+) are the 1:1 complexes and (2 × L1 + Li^+) and (2 × L2 + Li^+) are the 2:1 complexes. In Figure 3, the intensities of the complexes containing [5.5.5] are seen to be about twice that of the intensities of those containing [5.5.4], indicating the greater Li^+ affinity of [5.5.5] in both the 1:1 and 2:1 complexes. Table 3 summarizes these results. On the basis of comparison of the signal intensities in this manner, the overall trend in Li^+ binding affinity is: [5.5.5] > [5.5.4] > [4.4.4] > [5.5.3] > [5.4.3] > [4.4.3] > [1.1.1] > [3.3.1]. This trend generally correlates with two properties of the ligands—their cavity sizes and their polarizabilities. The ligand with the greatest Li^+ affinity, [5.5.5], is the most polarizable (see polarizability values in Table 2), meaning it has the greatest ability to stabilize the cationic charge. The Li^+ affinity of [4.4.4] is greater than that of [5.4.3], an interesting result because these two ligands have the same molecular weight and nominal size. This observation suggests that the symmetrical structure of [4.4.4] may allow more favorable overlap of the dipoles associated with the ether oxygens with the alkali metal relative to the more skewed overlap of the dipoles associated with the three different ether oxygens of [5.4.3]. The size of the ligand and the resulting polarizability alone cannot entirely account for the relative Li^+ affinities, as illustrated by the comparison of the relative Li^+ affinities of [4.4.4] and [5.5.3]. The ESI-MS analysis of the solution containing LiCl with [4.4.4] (nominal mass 268) and [5.5.3] (nominal mass 282) indicates that [4.4.4] has a greater Li^+ affinity by a factor of 7 relative to that of [5.5.3] (Table 3), despite the greater size of [5.5.3]. This result may indicate a more optimal overlap of the dipoles associated with the oxygen ether atoms of [4.4.4] with Li^+ due to the symmetry of [4.4.4] relative to that of [5.5.3].

The fourth type of experiment involved the use of collisional activated dissociation, a controlled fragmentation method, to break up the mixed-ligand/Li^+ complexes of the type (L1 + Li^+ + L2) where L1 and L2 represent two different ligands. This is an application of the "kinetic method", a technique commonly used to determine the relative gas-phase cation binding affinities of organic compounds.[12] The mixed ligand complexes (also termed "heterodimers") dissociate by loss of either L1 or L2, and the preference for the loss of L1 versus L2 gives a relative measurement of the lithium binding affinities of L1 and L2. An example is shown in Figure 4 for the ([5.5.5] + Li^+ + [5.5.4]) complex, and the other results are summarized in Table 4. The preferential loss of [5.5.4] from the ([5.5.5] + Li^+ + [5.5.4])$^+$ complex indicates that the [5.5.4] ligand is more weakly bound in the complex and thus has an Li^+ affinity lower than that of [5.5.5]. On the basis of the preferred dissociation pathways of all of the mixed-ligand 2:1 complexes listed in Table 4, it is evident that [5.5.5] has the greatest gas-phase Li^+ affinity, followed by [5.5.4], and [1.1.1] has the lowest Li^+ affinity among the ligands that formed stable 2:1 complexes. The overall trend in Li^+ affinities is [5.5.5] > [5.5.4] > [4.4.4] > [5.5.3] > [5.4.3] > [4.4.3] > [1.1.1] > [3.3.1],], a trend that parallels the order obtained for the Li^+ affinities of the ligands in solution obtained by ESI-MS analysis of solutions containing two ligands with LiCl (see Table 3). Apparently [5.5.5], with its suitable cavity size for Li^+ and its large polarizability effective for stabilizing cationic charge, is the best Li^+ ionophore.

Summary

Ring size effects significantly influence the capacity of the inositol-derived trispirocyclic ethers prepared herein for binding to alkali metal ions. Whereas the level of scaffold preorganization is closely similar through the series, the variations in conformational flexibility, the alterations in oxygen atom polarizability at the binding centers, and other elements of tunable structural control clearly play a critical, fundamental role in dictating receptor potential. Our experiments indicate that the [5.5.5] ionophore **1a** has the greatest Li^+/Na^+ selectivity and the greatest affinity for Li^+. Molecular symmetry appears to offer a thermodynamic and kinetic advantage when present. These findings might be construed to conform to the size-fit concept,[28] but evaluation of this basis is too approximative to be of value. Other factors are clearly of importance. For example, peripheral modifications force the oxygen atoms to adopt orientations more or less conducive to metal ion binding capability. An inability to attain an endodentate position obviously works to offset the benefits of preorganization. In addition, the selectivity and magnitude of the complexation behavior are dependent on the basicity and polarizability of the heteroatoms around the perimeter of the binding cavity.[29] These parameters, as well as other chemical interactions that may be operative, give new direction to the subject of molecular recognition.

Experimental Section

General. THF and ether were distilled from sodium/benzophenone ketyl under nitrogen just prior to use. For CH_2Cl_2, the drying agent was calcium hydride. All reactions were undertaken under a N_2 atmosphere. All aqueous extractions involved the use of triply distilled water. Analytical thin-layer chromatography was carried out on E. Merck silica gel 60 F_{254} aluminum-backed plates. All chromatographic purifications were performed on E. Merck silica gel 60 (230−400 mesh) using the indicated solvent systems. Melting points are uncorrected. ^1H and ^{13}C NMR spectra were recorded on Bruker instruments at 300 and 75 MHz, respectively. Elemental analyses were determined at Atlantic Microlab, Inc., Norcross, GA. The organic extracts were dried over anhydrous $MgSO_4$. The high-resolution mass spectra were recorded at The Ohio State University Campus Chemical Instrumentation Center.

Monoepoxide 11. The synthesis of **10** was improved as follows. To a clear solution of IBX (14.8 g, 53.0 mmol) in DMSO (100 mL) was added the known alcohol (19.0 g, 48.2 mmol) dissolved in CH_2Cl_2 (150 mL), and the mixture was stirred at

(28) Pedersen, C. J.; Frensdorff, H. K. *Angew. Chem., Int. Ed. Engl.* **1972**, *11*, 16.
(29) Miller, K. J. *J. Am.Chem. Soc.* **1990**, *112*, 8533.

Table 3. Lithium Selectivities by ESI-MS[a]

ligands + LiCl	dominant (1:1) complex	dominant (2:1) complex	selectivity
[5.5.5] [5.5.4]	([5.5.5] + Li)$^+$	(2[5.5.5] + Li)$^+$	[5.5.5] > [5.5.4], 2:1
[5.5.5] [5.5.3]	([5.5.5] + Li)$^+$	(2[5.5.5] + Li)$^+$	[5.5.5] >> [5.5.3], 55:1
[5.5.5] [4.4.4]	([5.5.5] + Li)$^+$	(2[5.5.5] + Li)$^+$	[5.5.5] > [4.4.4], 6:1
[5.5.5] [4.4.3]	([5.5.5] + Li)$^+$	(2[5.5.5] + Li)$^+$	[5.5.5] >>> [4.4.3], 1000:1
[5.5.5] [5.4.3]	([5.5.5] + Li)$^+$	(2[5.5.5] + Li)$^+$	[5.5.5] >>> [5.4.3], 1000:1
[5.5.5] [1.1.1]	([5.5.5] + Li)$^+$	(2[5.5.5] + Li)$^+$	[5.5.5] >>> [1.1.1], 1000:1
[5.5.4] [5.5.3]	([5.5.4] + Li)$^+$	(2[5.5.4] + Li)$^+$	[5.5.4] >> [5.5.3], 160:1
[5.5.4] [4.4.4]	([5.5.4] + Li)$^+$	(2[5.5.4] + Li)$^+$	[5.5.4] >> [4.4.4], 20:1
[5.5.4] [4.4.3]	([5.5.4] + Li)$^+$	(2[5.5.4] + Li)$^+$	[5.5.4] >>> [4.4.3], >1000:1
[5.5.4] [5.4.3]	([5.5.4] + Li)$^+$	(2[5.5.4] + Li)$^+$	[5.5.4] >>> [5.4.3], >1000:1
[5.5.4] [1.1.1]	([5.5.4] + Li)$^+$	(2[5.5.4] + Li)$^+$	[5.5.4] >>> [1.1.1], >1000:1
[5.5.3] [4.4.4]	([4.4.4] + Li)$^+$	(2[4.4.4] + Li)$^+$	[4.4.4] > [5.5.3], 7:1
[5.5.3] [4.4.3]	([5.5.3] + Li)$^+$	(2[5.5.3] + Li)$^+$	[5.5.3] > [4.4.3], 8:1
[5.5.3] [3.3.1]	([5.5.3] + Li)$^+$	(2[5.5.3] + Li)$^+$	[5.5.3] >>> [3.3.1], 1000:1
[5.5.3] [5.4.3]	([5.5.3] + Li)$^+$	(2[5.5.3] + Li)$^+$	[5.5.3] > [5.4.3], 3:1
[5.5.3] [1.1.1]	([5.5.3] + Li)$^+$	(2[5.5.3] + Li)$^+$	[5.5.3] >> [1.1.1], 25:1
[4.4.4] [4.4.3]	([4.4.4] + Li)$^+$	(2[4.4.4] + Li)$^+$	[4.4.4] >>> [4.4.3], >1000:1
	([4.4.4] + Na)$^+$	(2[4.4.4] + Na)$^+$	
[4.4.4] [5.4.3]	undistinguishable (same masses)		
[4.4.4] [1.1.1]	([4.4.4] + Li)$^+$	(2[4.4.4] + Li)$^+$	[4.4.4] >> [1.1.1], 100:1
[4.4.3] [5.4.3]	([5.4.3] + Li)$^+$	(2[5.4.3] + Li)$^+$	[5.4.3] > [4.4.3], 2:1
[4.4.3] [1.1.1]	([4.4.3] + Li)$^+$	(2[4.4.3] + Li)$^+$	[4.4.3] > [1.1.1], 7:1
[4.4.3] [1.1.1]	([4.4.3] + Li)$^+$	(2[4.4.3] + Li)$^+$	[4.4.3] > [1.1.1], 7:1
[3.3.1] [1.1.1]	([1.1.1] + Li)$^+$	none	[1.1.1] >> [3.3.1], >1000:1
[5.4.3] [1.1.1]	([5.4.3] + Li)$^+$	(2[5.4.3] + Li)$^+$	[5.4.3] > [1.1.1], 13:1

[a] Based on ESI-MS of solutions containing two ligands with LiCl, then measuring the intensities of the resulting Li^+ complexes.

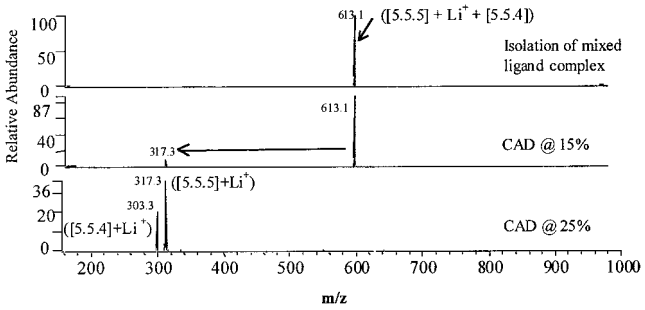

Figure 4. ESI-mass spectrum showing the isolation of the mixed-ligand complex, ([5.5.5] + Li^+ + [5.5.4]), followed by CAD at two energy settings.

Table 4. CAD Results for the Dissociation of the Mixed-Ligand Complexes (L1 + Li^+ + L2)[a]

complex (L1 + Li^+ + L2)	fragment (L1 + Li)$^+$	fragment (L2 + Li)$^+$	order of affinity
([5.5.5] + Li^+ + [5.5.4])	62	38	[5.5.5] > [5.5.4]
([5.5.5] + Li^+ + [5.5.3])	100	0	[5.5.5] >> [5.5.3]
([5.5.5] + Li^+ + [4.4.4])	85	15	[5.5.5] > [4.4.4]
([5.5.5] + Li^+ + [4.4.3])	100	0	[5.5.5] >> [4.4.3]
([5.5.5] + Li^+ + [5.4.3])	100	0	[5.5.5] >> [5.4.3]
([5.5.4] + Li^+ + [5.5.3])	100	0	[5.5.4] >> [5.5.3]
([5.5.4] + Li^+ + [4.4.4])	78	22	[5.5.4] > [4.4.4]
([5.5.3] + Li^+ + [4.4.4])	17	83	[4.4.4] > [5.5.3]
([5.5.3] + Li^+ + [4.4.3])	80	20	[5.5.5] > [4.4.3]
([5.5.3] + Li^+ + [5.4.3])	65	35	[5.5.3] > [5.4.3]
([5.5.3] + Li^+ + [1.1.1])	83	17	[5.5.3] > [1.1.1]
([4.4.3] + Li^+ + [5.4.3])	35	65	[5.4.3] > [4.4.3]
([5.4.3] + Li^+ + [1.1.1])	93	7	[5.4.3] > [1.1.1]

[a] Based on CAD results at 20% collision energy, reported as percentages of fragment ions scaled to 100%.

room temperature for 15 h. After dilution with CH_2Cl_2 (200 mL) and water (500 mL), the precipitate was filtered off. The filtrated was extracted with 1:1 CH_2Cl_2/hexanes, and the combined organic phases were washed with water and brine prior to drying. The concentrate was subjected to flash chromatography on silica gel (elution with 20% ethyl acetate in hexanes) to give **10** as a white solid (17.4 g, 92%), mp 63−64 °C (lit.[6c] mp 62−64 °C).

To a clear solution of trimethylsulfoxonium iodide (10.7 g, 48.7 mmol) in DMSO (100 mL) was added sodium hydride (1.27 g of 60% in oil, 53.1 mmol), and the mixture was stirred for 40 min prior to the introduction of **10** (17.4 g, 44.3 mmol) in THF (100 mL) via cannula. The reaction mixture was stirred for 1 h, quenched with cold water, and extracted with 1:1 CH_2Cl_2/hexanes. The combined organic layers were washed with water and brine prior to drying and concentration. The residue was flash chromatographed on silica gel (elution with 20% ethyl acetate in hexanes) to give **11** as a white solid, mp 99.5−100.5 °C (15.4 g, 86%): IR (neat, cm^{-1}) 1254, 1163, 1118; ^{1}H NMR (300 MHz, $CDCl_3$) δ 7.33 (m, 5 H), 5.60 (d, J = 1.1 Hz, 1 H), 4.66 (d, J = 12.0 Hz, 1 H), 4.53 (d, J = 12.0 Hz, 1 H), 4.27 (m, 1 H), 4.14 (m, 1 H), 3.78 (m, 1 H), 3.53 (m, 1 H), 2.88 (d, J = 4.6 Hz, 1 H), 2.85 (d, J = 4.6 Hz, 1 H), 0.91 (s, 9 H), 0.11 (s, 6 H); ^{13}C NMR (75 MHz, $CDCl_3$) δ 137.3, 128.5 (2C), 128.0, 127.6 (2C), 103.3, 76.3, 72.8, 72.6, 71.4, 71.3, 65.8, 63.6, 25.8 (3C), 18.3, 15.2, −4.7 (2C); EI MS m/z (M^+) calcd 406.1812, obsd 406.1800. Anal. Calcd for $C_{21}H_{30}O_6Si$: C, 62.04; H, 7.44. Found: C, 62.16; H, 7.42.

Epoxy Alcohol 12. A cold (0 °C) solution of **11** (12.0 g, 29.5 mmol) in THF (100 mL) was treated with TBAF (32.5 mmol) in THF (30 mL). The stirred reaction mixture was allowed to warm to room temperature during 2 h, concentrated, diluted with water, and extracted with ethyl acetate. The combined organic phases were washed with water and brine prior to drying and solvent evaporation. Flash chromatography of the residue on silica gel (elution with 50% ethyl acetate in hexanes containing 1% methanol) furnished 8.40 g (97%) of **12** as a white solid, mp 123−124 °C: IR (neat, cm^{-1}) 3220, 1160, 1120; ^{1}H NMR (300 MHz, $CDCl_3$) δ 7.34 (m, 5 H), 5.58 (s, 1 H), 4.67 (d, J = 11.7 Hz, 1 H), 4.53 (d, J = 11.7 Hz, 1 H), 4.34 (m, 1 H), 4.26 (m, 1 H), 4.15 (d, J = 11.0 Hz, 1 H), 3.84 (m, 1 H), 3.64 (m, 1 H), 3.17 (d, J = 11.7 Hz, 1 H), 2.90 (d, J = 4.6 Hz, 1 H), 2.87 (d, J = 4.6 Hz, 1 H); ^{13}C NMR (75 MHz, $CDCl_3$) δ 137.1, 128.6 (2C), 128.1, 127.7 (2C), 103.5, 76.1, 72.5, 72.1, 71.4, 71.2, 63.2, 54.7, 50.4; EI MS m/z (M^+) calcd 292.0947, obsd 292.0946. Anal. Calcd for $C_{15}H_{16}O_6$: C, 61.64; H, 5.52. Found: C, 61.53; H, 5.58.

Diepoxide 14. Dimethyl sulfoxide (8.98 g, 115 mmol) was added to a cold (−78 °C) solution of oxalyl chloride (7.30 g, 57.5 mmol) in CH_2Cl_2 (100 mL) during 5 min, and the reaction mixture was stirred for 15 min prior to the introduction of **12** (8.40 g, 28.7 mmol) dissolved in CH_2Cl_2 (100 mL) at 0 °C. After the reaction mixture had been stirred at −78 °C for 2 h,

triethylamine (14.6 g, 144 mmol) was added dropwise via syringe, and stirring was maintained for 1 h with concurrent slow warm to room temperature. Water was added, the product was taken up in CH_2Cl_2/hexanes (1:1), and the combined organic phases were washed with water and brine prior to drying and concentration. The ketone **13** so generated was directly subjected to the next reaction.

To a clear solution of trimethylsulfoxonium iodide (6.64 g, 30.2 mmol) in DMSO (70 mL) was added sodium hydride (0.73 g of 95%, 30.2 mmol), and the reaction mixture was stirred for 40 min before being treated via cannula with a solution of the above ketone **13** (8.34 g, 28.7 mmol) in THF (50 mL). After an additional 1 h, the mixture was diluted with water and CH_2Cl_2. The combined organic phases were washed with water and brine, dried, and concentrated prior to chromatography of the residue on silica gel (elution with 20% ethyl acetate in 1:1 CH_2Cl_2/hexanes) to give **14** (5.85 g, 67% over two steps). Careful purification at this stage is necessary for the ensuing debenzylation reaction to succeed; white solid, mp 184−185 °C; IR (neat, cm^{-1}) 1363, 1281, 1158; ^1H NMR (300 MHz, $CDCl_3$) δ 7.34 (m, 5 H), 5.72 (s, 1 H), 4.65 (s, 2 H), 4.35 (m, 1 H), 3.95 (m, 2 H), 3.26 (m, 1 H), 2.87 (d, J = 4.5 Hz, 2 H), 2.82 (d, J = 4.5 Hz, 1 H); ^{13}C NMR (75 MHz, $CDCl_3$) δ 137.3, 128.7 (2C), 128.1, 128.0 (2C), 103.6, 76.5, 72.3 (2C), 72.1, 71.1, 54.4 (2C), 49.9 (2C); EI MS m/z (M^+) calcd 304.0946, obsd 304.0938. Anal. Calcd for $C_{16}H_{16}O_6$: C, 63.15; H, 5.30. Found: C, 62.86; H, 5.37.

Diepoxy Alcohol 15. A solution of **14** (1.52 g, 5.00 mmol) in 150 mL of ethyl acetate containing $PdO{\cdot}xH_2O$ (150 mg) was hydrogenolyzed under 1 atm of H_2. After 1 h, the solution, which had become a white turbid suspension, was diluted with CH_2Cl_2 and filtered through a pad of diatomaceous earth. After evaporation of the filtrate and crystallization from 1:1 CH_2Cl_2/hexanes, there was isolated 1.01 g (94%) of **15** as a white solid, mp 244−246 °C: IR (neat, cm^{-1}) 3314, 1142; ^1H NMR (300 MHz, $CDCl_3$) δ 5.74 (s, 1 H), 4.54 (dt, J = 10.5, 3.8 Hz, 1 H), 3.92 (dd, J = 3.8, 1.8 Hz, 2 H), 3.29 (t, J = 1.8 Hz, 1 H), 2.95 (d, J = 4.3 Hz, 2 H), 2.90 (d, J = 4.3 Hz, 2 H), 2.70 (d, J = 10.5 Hz, 1 H); ^{13}C NMR (75 MHz, $CDCl_3$) δ 102.8, 75.0, 73.1, 68.0, 54.4, 50.0; ES MS m/z $(M + Na)^+$ calcd 237.0375, obsd 237.0375. Anal. Calcd for $C_9H_{10}O_6$: C, 50.47; H, 4.71. Found: C, 50.50; H, 4.70.

Diepoxy Hemiacetal 16. A mixture of **15** (400 mg, 1.87 mmol), NMO (328 mg, 2.80 mmol), and 4 Å MS (930 mg) in dry acetonitrile was stirred for 30 min before TPAP (33 mg, 0.093 mmol) was introduced. After 3 h, CH_2Cl_2 was added, and filtration was performed through a pad of diatomaceous earth. The filtrate was concentrated, the residue was chromatographed on silica gel (elution with 3% methanol in CH_2Cl_2), and the eluate was further purified by trituration with 1:1 CH_2Cl_2/hexanes to give **16** (370 mg, 81%) as a white solid, mp >280 °C; ^1H NMR (300 MHz, DMSO-d_6) δ 6.43 (s, 1 H), 5.81 (s, 1 H), 3.69 (d, J = 1.5 Hz, 2 H), 3.26 (s, 1 H), 3.21 (s, 3 H), 2.87 (d, J = 5.1 Hz, 2 H), 2.81 (d, J = 5.1 Hz, 2 H); ^{13}C NMR (75 MHz, DMSO-d_6) δ 102.6, 91.3, 75.0, 73.4, 55.1, 48.6, 47.2; EI MS m/z $(M - CH_3OH)^+$ calcd 212.0332, obsd 212.0328. Anal. Calcd for $C_{10}H_{12}O_7$: C, 49.18; H, 4.95. Found: C, 48.66; H, 4.86.

Triepoxide 3. To a clear solution of trimethylsulfoxonium iodide (348 mg, 1.58 mmol) in DMSO (5 mL) was added Triton B (40% solution, 1.32 g, 3.15 mmol), and the reaction mixture was stirred for 40 min prior to the addition via cannula of a solution of **16** (350 mg, 1.43 mmol) in THF (10 mL). The reaction mixture was stirred for 1 h, treated with saturated NH_4Cl solution until neutrality was achieved, and freed of DMSO by direction of a stream of air at the sample. The residue was slurried with silica gel and CH_2Cl_2 and purified by flash chromatography (silica gel, elution with 1% methanol in ethyl acetate) to provide 165 mg (51%) of **3** as a white solid, mp >280 °C: IR (neat, cm^{-1}) 1059, 1031; ^1H NMR (300 MHz, DMSO-d_6) δ 6.03 (s, 1 H), 3.52 (s, 3 H), 2.93 (s, 6 H); ^{13}C NMR (75 MHz, DMSO-d_6) δ 102.6, 74.2, 55.1, 49.5; EI MS m/z (M^+) calcd 226.0477, obsd 226.0468.

Diepoxy Methyl Ether 5. A mixture of **15** (300 mg, 1.40 mmol) and sodium hydride (59 mg of 60% in oil, 1.54 mmol) in DMF (10 mL) was stirred for 20 min prior to the introduction of methyl iodide (218 mg, 1.54 mmol). After 13.5 h of stirring, saturated NH_4Cl solution (5 mL) was added followed by water. The product was extracted into CH_2Cl_2, and the combined organic phases were washed with water and brine prior to drying and solvent evaporation. The concentrate was subjected to careful flash chromatography (silica gel, elution with 20% ethyl acetate in 1:1 CH_2Cl_2/hexanes) to afford **5** (289 mg, 91%) as a white solid, mp 230−232 °C: IR ($CHCl_3$, cm^{-1}) 1157, 1001; ^1H NMR (300 MHz, $CDCl_3$) δ 5.74 (s, 1 H), 4.20 (t, J = 3.7 Hz, 1 H), 3.99 (dd, J = 2.6, 1.7 Hz, 2 H), 3.48 (s, 3 H), 3.23 (s, 1 H), 2.88 (d, J = 4.4 Hz, 2 H), 2.82 (d, J = 4.4 Hz, 2 H); ^{13}C NMR (75 MHz, $CDCl_3$) δ 103.2, 76.0, 74.6, 71.7, 57.4, 54.1, 49.6; ES MS m/z $(M + Na)^+$ calcd 251.0532, obsd 251.0538. Anal. Calcd for $C_{10}H_{12}O_6$: C, 52.63; H, 5.30. Found: C, 52.74; H, 5.27.

Dioxetane Benzyl Ether 17. To a clear solution of trimethylsulfoxonium iodide (5.18 g, 23.5 mmol) in DMSO (30 mL) was added sodium hydride (0.57 g of 95%, 23.5 mmol). After 40 min of stirring, diepoxide **14** (2.05 g, 6.72 mmol) dissolved in 30 mL of THF was introduced via cannula, and the mixture was stirred for 1 h prior to dilution with CH_2Cl_2 and water. The aqueous phase was extracted with 1:1 CH_2Cl_2/hexanes, and the combined organic phases were washed with water and brine prior to drying. The concentrate was purified by careful flash chromatography on silica gel (elution with ethyl acetate then 1% methanol in CH_2Cl_2) to provide 1.41 g (63%) of **17**. Once again, careful purification is important for the success of the subsequent debenzylation; white solid, mp 143−144 °C; IR (neat, cm^{-1}) 1149; ^1H NMR (300 MHz, $CDCl_3$) δ 7.30 (m, 5 H), 5.28 (s, 1 H), 4.71 (m, 4 H), 4.61 (m, 3 H), 4.43 (m, 2 H), 4.33 (m, 1 H), 2.81 (t, J = 8.1 Hz, 4 H); ^{13}C NMR (75 MHz, $CDCl_3$) δ 137.7, 128.4 (2C), 128.0 (2C), 127.7, 102.1, 80.6, 76.8, 73.2, 72.0, 71.3, 67.3, 31.9; EI MS m/z (M^+) calcd 332.1260, obsd 332.1266. Anal. Calcd for $C_{18}H_{20}O$: C, 65.05; H, 6.07. Found: C, 65.16; H, 6.02.

Dioxetanyl Alcohol 18. A solution of **17** (740 mg, 2.23 mmol) in ethyl acetate (30 mL) containing 80 mg of $Pd(O){\cdot}xH_2O$ was hydrogenolyzed under 1 atm of H_2 for 3 h. Following dilution with CH_2Cl_2, the mixture was filtered through diatomaceous earth, and the filtrate was evaporated to give 540 mg (100%) of **18** as a white solid, mp 117−118 °C: IR (neat, cm^{-1}) 3519, 1151, 1037; ^1H NMR (300 MHz, $CDCl_3$) δ 5.29 (s, 1 H), 4.74 (m, 4 H), 4.58 (br s, 1 H), 4.48 (m, 3 H), 3.25 (br s, 1 H), 2.81 (m, 4 H); ^{13}C NMR (75 MHz, $CDCl_3$) δ 101.5, 81.7, 76.7, 72.4, 68.8, 68.6, 31.8; EI MS m/z (M^+) calcd 242.0790, obsd 242.0795. Anal. Calcd for $C_{11}H_{14}O_6$: C, 54.54; H, 5.83. Found: C, 54.55; H, 5.82.

Trioxetane 4. A mixture of **18** (950 mg, 3.92 mmol), NMO (920 mg, 7.84 mmol), and 4 Å MS (2 g) in CH_2Cl_2 (40 mL) was stirred for 20 min before TPAP (69 mg, 0.20 mmol) was introduced. After 3 h of stirring, dilution was made with CH_2Cl_2 in advance of filtration through diatomaceous earth. The filtrate was concentrated, and the residue was subjected to flash chromatography on silica gel (elution with 2% methanol in CH_2Cl_2) to give a 1.6:1 mixture (^1H NMR analysis) of **19** and **20** as a pale brown viscous oil (850 mg, 85%).

Exposure of this mixture (400 mg, 1.56 mmol) in THF (10 mL) to trimethylsulfoxonium iodide (1.37 g, 6.24 mmol) in DMSO (15 mL) containing sodium hydride (300 mg of 60% in oil, 7.80 mmol) for 12 h and workup in the predescribed fashion gave a crude product that was purified by flash chromatography on silica gel (elution with 2−5% methanol in CH_2Cl_2) to afford 205 mg (49%) of **4** as a white solid, mp 269−272 °C: IR (neat, cm^{-1}) 1151, 1032; ^1H NMR (300 MHz, $CDCl_3$) δ 5.23 (s, 1 H), 4.73 (t, J = 8.0 Hz, 6 H), 4.60 (s, 3 H), 2.84 (t, J = 8.0 Hz, 6 H); ^{13}C NMR (75 MHz, $CDCl_3$) δ 101.7, 81.2, 76.1, 67.7, 31.6; EI MS m/z (M^+) calcd 268.0946, obsd 268.0956.

Dioxetanyl Epoxide 6. A clear solution of trimethylsulfoxonium iodide (416 mg, 1.89 mmol) in DMSO (5 mL) was treated with Triton B (1.58 mg of 40%, 3.78 mmol) and stirred for 30 min. A 440 mg (1.74 mmol) sample of **19** dissolved in THF (10 mL) was introduced via cannula, and the mixture was stirred for 1.5 h before being diluted with water and CH_2Cl_2. The aqueous phase was extracted with 1:1 CH_2Cl_2/

hexanes, and the combined organic phases were evaporated to leave a residue that was subjected to flash chromatography on silica gel (elution with 2% methanol in CH_2Cl_2). There was isolated 280 mg (63%) of **6** as a white solid, mp 206−207 °C: IR (neat, cm^{-1}) 1149, 1039; ^1H NMR (300 MHz, $CDCl_3$) δ 5.46 (s, 1 H), 4.78−4.61 (series of m, 5 H), 3.92 (d, J = 1.8 Hz, 2 H), 2.93−2.78 (series of m, 6 H); ^{13}C NMR (75 MHz, $CDCl_3$) δ 102.2, 80.8, 76.8, 75.3, 67.5, 53.6, 48.5, 30.9; EI MS m/z (M^+) calcd 254.0790, obsd 254.0784. Anal. Calcd for $C_{12}H_{14}O_6$: C, 56.69; H, 5.55. Found: C, 56.78; H, 5.59.

Benzyloxy Tetrahydrofuranyl Alcohol 22. The known ketone **10** was homologated by reaction with the Normant reagent to provide the known 1,4-diol. A mixture of this diol (13.5 g, 29.8 mmol), *p*-toluenesulfonyl chloride (11.4 g, 60.0 mmol), triethylamine (12.1 g, 120 mmol), and DMAP (184 mg, 1.50 mmol) in ethylene dichloride (200 mL) was stirred at 20 °C for 15 h and at 70 °C for an additional 7 h. The cooled reaction mixture was diluted with water, and the separated organic phase was extracted with 1:1 CH_2Cl_2/hexanes. The combined organic layers were washed with water and brine prior to drying and solvent evaporation. The residue was subjected to flash chromatography on silica gel (elution with 20% ethyl acetate in hexanes) to give the cyclized ether as a tan oil (11.2 g), which was immediately subjected to further reaction.

The above oil (11.2 g) was dissolved in THF (30 mL), cooled to 0 °C, treated with a solution of TBAF (19.5 g, 74.7 mmol) in THF (70 mL), and stirred for 2 h with slow warming to room temperature. Solvent evaporation was followed by the addition of water to the concentrate. The product was extracted into CH_2Cl_2, and the combined organic layers were washed with water and brine, dried, and freed of solvent. Flash chromatography of the residue on silica gel (elution with 30% → 50% ethyl acetate in hexanes containing 1% methanol) furnished 8.20 g (86%) of **22** as a pale yellow oil: IR (neat, cm^{-1}) 3470; ^1H NMR (300 MHz, $CDCl_3$) δ 7.36−7.27 (series of m, 5 H), 5.43 (s, 1 H), 4.68 (d, J = 11.9 Hz, 2 H), 4.57 (d, J = 11.9 Hz, 2 H), 4.31 (t, J = 3.6 Hz, 1 H), 4.18 (br s, 1 H), 4.14 (m, 1 H), 3.98−3.93 (series of m, 3 H), 3.96 (m, 1 H), 2.28 (m, 2 H), 1.94 (m, 2 H); ^{13}C NMR (75 MHz, $CDCl_3$) δ 137.7, 128.4, 127.8, 127.6, 103.2, 79.8, 76.6, 73.6, 72.6, 72.2, 71.2, 69.6, 62.5, 35.1, 24.5; EI MS m/z (M^+) calcd 320.1260, obsd 320.1273. Anal. Calcd for $C_{17}H_{20}O_6$: C, 63.74; H, 6.29. Found: C, 63.47; H, 6.32.

Benzyloxytetrahydrofuranyl Ketone 23. DMSO (7.91 g, 101 mmol) was added to a cold (−78 °C) solution of oxalyl chloride (6.42 g, 50.6 mmol) in CH_2Cl_2 (100 mL) during 5 min, and the reaction mixture was stirred for 15 min before a solution of **22** (8.10 g, 25.3 mmol) in cold (0 °C) CH_2Cl_2 (100 mL) was introduced. After 2 h of stirring at −78 °C, triethylamine (12.8 g, 126.5 mmol) was introduced dropwise via syringe, and the mixture was allowed to warm slowly to 20 °C during 1 h. Water was added and the product was taken up in 1:1 CH_2Cl_2/hexanes. The combined organic phases were washed with water and brine prior to drying and concentration. The residue was purified by flash chromatography on silica gel (elution with 25% → 50% ethyl acetate in hexanes) to give **23** as a viscous pale green oil (6.91 g, 85%): IR (neat, cm^{-1}) 1764, 1156; ^1H NMR (300 MHz, $CDCl_3$) δ 7.35−7.27 (series of m, 5 H), 5.62 (s, 1 H), 4.64 (d, J = 12.2 Hz, 1 H), 4.59 (d, J = 12.2 Hz, 1 H), 4.48 (t, J = 3.6 Hz, 1 H), 4.33 (m, 1 H), 4.08 (m, 1 H), 3.96 (m, 3 H), 2.38 (m, 1 H), 2.28 (m, 1 H), 1.94 (m, 2 H); ^{13}C NMR (75 MHz, $CDCl_3$) δ 199.6, 137.0, 128.4, 127.9, 127.7, 102.4, 83.2, 81.0, 77.1, 75.5, 73.1, 71.2, 70.0, 35.0, 24.2; EI MS m/z (M^+) calcd 318.1103, obsd 318.1136.

Benzyloxytetrahydrofuranyl Oxetane 24. A solution of trimethylsulfoxonium iodide (1.82 g, 8.25 mmol) in DMSO (15 mL) was treated with sodium hydride (316 mg of 60% in oil, 8.25 mmol) and stirred for 40 min to give a clear solution. A solution of **23** (750 mg, 2.36 mmol) in THF (10 mL) was added via cannula, and the mixture was stirred for 15 h, quenched with water, and extracted with 1:1 CH_2Cl_2/hexanes. The combined organic layers were washed with water and brine prior to solvent evaporation. Flash chromatography of the residue on silica gel (gradient elution with 50% ethyl acetate in hexanes to 100% ethyl acetate) to provide 428 mg (52%) of **24** as a white solid, mp 106−107 °C: IR (neat, cm^{-1}) 1164, 1146; ^1H NMR (300 MHz, $CDCl_3$) δ 7.43−7.28 (series of m, 5 H), 5.33 (s, 1 H), 4.70 (d, J = 12.6 Hz, 1 H), 4.65 (d, J = 12.6 Hz, 1 H), 4.62 (t, J = 7.9 Hz, 2 H), 4.42 (m, 1 H), 4.29 (t, J = 3.4 Hz, 1 H), 4.10−3.88 (series of m, 4 H), 2.78 (dt, J = 2.2, 7.9 Hz, 2 H), 2.26 (m, 2 H), 1.93 (m, 2 H); ^{13}C NMR (75 MHz, $CDCl_3$) δ 137.9, 128.3, 127.9, 127.6, 102.3, 80.4, 78.9, 76.9, 73.4, 72.4, 71.5, 71.2, 69.6, 66.8, 36.1, 32.0, 24.1; ES MS m/z ($M + Na)^+$ calcd 369.1314, obsd 369.1317. Anal. Calcd for $C_{19}H_{22}O_6$: C, 65.88; H, 6.40. Found: C, 65.85; H, 6.44.

Hydroxytetrahydrofuranyl Oxetane 25. A solution of **24** (360 mg, 1.04 mmol) in ethyl acetate (20 mL) was hydrogenolyzed in the presence of $PdO{\cdot}xH_2O$ (25 mg) under 1 atm of H_2 for 1 h. The reaction mixture was diluted with CH_2Cl_2, filtered through diatomaceous earth, and freed of solvent. There was isolated 255 mg (96%) of **25** as a white solid, mp 106−108 °C: IR (neat, cm^{-1}) 3504; ^1H NMR (300 MHz, $CDCl_3$) δ 5.37 (s, 1 H), 4.74 (m, 1 H), 4.64 (m, 1 H), 4.52 (m, 1 H), 4.45 (br s, 1 H), 4.09−3.92 (series of m, 5 H), 2.83 (t, J = 7.9 Hz, 2 H), 2.38 (m, 1 H), 2.21 (m, 1 H), 1.99 (m, 2 H); ^{13}C NMR (75 MHz, $CDCl_3$) δ 101.8, 81.5, 80.4, 76.9, 73.1, 71.5, 69.7, 68.4, 67.9, 35.6, 32.0, 24.0; ES MS m/z ($M + Na)^+$ calcd 279.0845, obsd 279.0854. Anal. Calcd for $C_{12}H_{16}O_6$: C, 56.25; H, 6.29. Found: C, 56.28; H, 6.39.

Ketotetrahydrofuranyl Oxetane 26. A mixture of **25** (200 mg, 0.78 mmol), NMO (183 mg, 1.56 mmol), and 4 Å molecular sieves (390 mg) in CH_2Cl_2 (20 mL) was stirred for 20 min and treated with TPAP (14 mg, 0.039 mmol). After 15 h of stirring, CH_2Cl_2 was added, and the mixture was filtered through a pad of diatomaceous earth and concentrated. Flash chromatography of the residue on silica gel (elution with ethyl acetate) provided 161 mg (78%) of **26** as a white solid, mp 180−182 °C: IR (neat, cm^{-1}) 1764, 1158; ^1H NMR (300 MHz, $CDCl_3$) δ 5.56 (s, 1 H), 4.63 (m, 2 H), 4.48 (t, J = 1.7 Hz, 1 H), 4.14 (t, J = 1.7 Hz, 1 H), 4.09−3.87 (series of m, 3 H), 2.96 (m, 1 H), 2.85 (m, 1 H), 2.43 (m, 1 H), 2.25 (m, 1 H), 1.98 (m, 2 H); ^{13}C NMR (75 MHz, $CDCl_3$) δ 199.2, 102.1, 83.5, 82.1, 80.6, 79.8, 77.7, 70.0, 67.3, 34.5, 30.7, 24.2; ES MS m/z ($M + Na)^+$ calcd 277.0688, obsd 277.0689. Anal. Calcd for $C_{12}H_{14}O_6$: C, 56.69; H, 5.55. Found: 56.39; H, 5.51.

Tetrahydrofuranyl Oxetanyl Epoxide 9. A solution of trimethylsulfoxonium iodide (286 mg, 1.30 mmol) in DMSO (3 mL) was treated with Triton B (217 mg of 40% in methanol, 1.30 mmol) and stirred for 40 min. A solution of **26** (300 mg, 1.18 mmol) in THF (8 mL) was next introduced via cannula, and the reaction mixture was stirred for 1 h prior to solvent evaporation. The residue was mixed with CH_2Cl_2 and water, and the aqueous phase was further extracted with CH_2Cl_2. The combined organic layers were washed with water, dried, and concentrated. Flash chromatographic purification of the residue on silica gel (elution first with ethyl acetate and then 1% methanol in ethyl acetate) gave 213 mg (67%) of **9** as a white solid, mp 170−171 °C: IR (neat, cm^{-1}) 1158, 1047; ^1H NMR (300 MHz, $CDCl_3$) δ 5.48 (s, 1 H), 4.60 (t, J = 7.9 Hz, 2 H), 4.15−3.80 (series of m, 4 H), 3.34 (m, 1 H), 2.78 (m, 4 H), 2.25 (m, 2 H), 1.95 (m, 2 H); ^{13}C NMR (75 MHz, $CDCl_3$) 102.5, 80.8, 79.6, 77.0, 75.8, 75.1, 69.5, 66.9, 54.2, 48.7, 35.0, 31.1, 24.3; ES MS m/z ($M + Na)^+$ calcd 291.0845, obsd 291.0837. Anal. Calcd for $C_{13}H_{16}O_6$: C, 58.20; H, 6.01. Found: C, 57.93; H, 6.03.

Bistetrahydrofuranyl Oxetane 8. A mixture of **26** (700 mg, 2.75 mmol) and dry lithium perchlorate (1.46 g, 13.8 mmol) in THF (50 mL) was stirred for 3 h at 20 °C, cooled to −78 °C, and treated dropwise with the Normant reagent (0.56 M in THF, 8.25 mmol). The reaction mixture was stirred for 1 h at −78 °C and for 1 h at −40 °C before solid NH_4Cl was introduced and filtration through diatomaceous earth was undertaken. The filtrated was evaporated and the residue was leached with 1:1 CH_2Cl_2/hexanes. The combined organic solutions were washed with water and brine, dried, and freed of solvent. The concentrate was subjected to flash chromatography on silica gel (elution with 30% → 50% ethyl acetate containing 3% → 5% methanol) to give the diol as a viscous colorless oil (620 mg, 72%).

A cold (0 °C) mixture of the crude diol (610 mg, 1.94 mmol), *p*-toluene-sulfonyl chloride (707 mg, 3.71 mmol), triethylamine (752 mg, 7.43 mmol), DMAP (15 mg, 0.12 mmol), and CH_2Cl_2 (20 mL) was stirred for 1.5 h with slow warming to room temperature. Water was introduced, and the product was extracted into CH_2Cl_2 (3 × 50 mL). The organic phase was washed with water (50 mL) and brine (50 mL) prior to drying and solvent evaporation. Flash chromatography of the residue (silica gel, elution with 25% → 50% ethyl acetate in hexanes) gave the monotosylate as a white foam (805 mg, 89%), which was directly submitted to the next reaction.

This tosylate (805 mg) was dissolved in benzene (20 mL), cooled to 0 °C, treated with potassium hexamethyldisilazide in toluene (0.4 M, 3.44 mmol) via syringe, and stirred for 1 h with slow warming to room temperature. Water was introduced, the product was extracted into CH_2Cl_2, and the combined organic phases were washed with water and filtered through a short pad of silica gel (elution with 5% methanol in CH_2Cl_2). Solvent evaporation furnished **8** (488 mg, 96% or 61% over 3 steps) as a white solid, mp 140−141 °C: IR (neat, cm^{-1}) 1153, 994; ^1H NMR (300 MHz, $CDCl_3$) δ 5.32 (s, 1 H), 4.55 (t, J = 7.9 Hz, 2 H), 4.04−3.91 (series of m, 6 H), 3.53 (m, 1 H), 2.77 (t, J = 7.9 Hz, 2 H), 2.25 (m, 4 H), 1.92 (m, 4 H); ^{13}C NMR (75 MHz, $CDCl_3$) δ 102.2, 81.2, 79.9, 76.0, 75.9, 69.3, 66.5, 35.9, 32.1, 24.0; ES MS m/z $(M + Na)^+$ calcd 319.1158, obsd 319.1152. Anal. Calcd for $C_{15}H_{20}O_6$: C, 60.80; H, 6.80. Found: C, 60.57; H, 6.87.

Bistetrahydrofuranyl Epoxide 7. A solution of trimethylsulfoxonium iodide (506 mg, 2.30 mmol) in DMSO (6 mL) was treated with Triton B (1.04 mL of 40% in methanol, 2.30 mmol) and stirred for 40 min prior to the addition via cannula of **27** (552 mg, 2.06 mmol) dissolved in THF (15 mL). The reaction mixture was stirred for 1 h and diluted with water and CH_2Cl_2. The aqueous phase was extracted with CH_2Cl_2, and the combined organic layers were washed with water, dried, and evaporated. Flash chromatography of the residue on silica gel (elution with 1:1 CH_2Cl_2/ethyl acetate) afforded **7** (360 mg, 62%) as a white solid, mp 217−218 °C: IR ($CHCl_3$, cm^{-1}) 1156, 1064; ^1H NMR (300 MHz, $CDCl_3$) δ 5.56 (s, 1 H), 4.06−3.91 (m, 4 H), 3.67 (t, J = 1.9 Hz, 1 H), 3.35 (d, J = 1.9 Hz, 2 H), 2.77 (s, 2 H), 2.38−2.18 (m, 4 H), 1.97−1.86 (m, 4 H); ^{13}C NMR (75 MHz, $CDCl_3$) δ 102.9, 79.9, 77.2, 75.7, 69.5, 54.6, 49.0, 35.4, 24.2; ES MS m/z $(M + Na)^+$ calcd 305.0996, obsd 305.0984. Anal. Calcd for $C_{14}H_{18}O_6$: C, 59.57; H, 6.43. Found: C, 59.46; H, 6.46.

Complexation Studies.[21] All glassware involved was base-washed and rinsed sequentially with acetone and distilled, demineralized water (2×) prior to drying. Host solutions were prepared in acid-free $CDCl_3$ in the 0.014−0.020 M concentration range. Experiments were conducted simultaneously on four to six samples of the identical polyether plus a blank. The mean value of the absorbance (A) was used in the calculations. Two or more determinations were carried out until good duplication was realized. All measurements of volume were done by difference. Volumes of <0.4 mL were transferred in Hamilton gastight syringes. Care was taken at all times to avoid evaporation of the $CDCl_3$ solutions.

To each of two graduated distillation receiver flasks containing a micro magnetic stirring bar was introduced the host solution (0.4 mL). A solution of the alkali metal picrate in water (0.5 mL) followed. The tubes were stoppered and placed in a water bath at 20 °C. The contents of the tubes were stirred as rapidly as possible for 5.0 min (stopclock) before centrifugation to produce two clear layers. For each tube, a 50- to 150-μL aliquot (depending on color intensity) of the chloroform layer was removed and transferred to a 5-mL volumetric flask. Dilution to the mark with CH_3CN produced solutions suitable for UV measurement. A blank sample was similarly prepared with 0.4 mL of host solution and 0.5 mL of demineralized water.

UV measurements were made on a Uvikon 930 spectrophotometer. The same cell was used as reference on each occasion, and the pair of cells were always oriented in the same way inside the spectrophotometer. The cells were "zeroed" in the instrument at 380 nm. The extraction constants (K_{ex}) were calculated using equilibrium eq 2 in ref 22 from the concentration of picrate salt measured in the original $CDCl_3$ layer. Correction for the water solubility of hosts was made by measurement of K_d for hosts ($CHCl_3/H_2O$) according to the literature method.[22]

^{13}C NMR Titration Studies. A solution of **8** (50 mg, 0.20 mmol) in 1:1 $CH_3CN/CDCl_3$ was placed in an NMR tube. A separate solution of $LiClO_4$ (32 mg, 0.30 mmol) in the same solvent system (1.2 mL) was prepared. A ^{13}C NMR spectrum was recorded after incremental addition of 0.20 mL (0.25 equiv) aliquots of the perchlorate salt up to 1.0 equiv of $LiClO_4$.

ESI-MS Experimental Details. All experiments were undertaken with a ThermoFinnigan LCQ-Duo ion trap mass spectrometer equipped with an electrospray ionization source. All solutions consisted of 99% chloroform with 1% methanol to solubilize the metal salts, admitted via a syringe pump at a flow rate of 10 μL/min. Desolvation of the complexes was facilitated by a heated capillary at 125 °C. The base pressure in the ion trap was nominally 8.9×10^{-6} T. The needle voltage was set at 4.5 kV. The concentrations of the ligands and metal salts were typically 1.0×10^{-5} M unless otherwise stated. The solutions were vortexed briefly prior to loading into the syringe pump. All of the metal salts were purchased as chloride salts from Aldrich Company. Twenty scans were averaged for each reported result. The ion trap was tuned on the (18-crown-6 + K^+) complex, and this tune file was used for all data acquisitions.

Acknowledgment. Funding from the National Science Foundation (CHE-9980672 to L.A.P; CHE-9820755 to J.S.B), the Welch Foundation (F-1155), and the Texas Advanced Technology Program (003659-0206) are gratefully acknowledged.

Supporting Information Available: X-ray crystallographic details for **3** and **4**. This material is available free of charge via the Internet at http://pubs.acs.org.

JO0107507